Article

Ballistic Performance of Raffia Fiber Fabric Reinforcing Epoxy Composites as Standalone Targets

Douglas Santos Silva *, Raí Felipe Pereira Junio, Marcelo Henrique Prado da Silva and Sergio Neves Monteiro

Department of Materials Science, Military Institute of Engineering—IME, Praça General Tibúrcio, 80, Praia Vermelha, Urca, Rio de Janeiro 22290-270, Brazil; raivsjfelipe@ime.eb.br (R.F.P.J.); marceloprado@ime.eb.br (M.H.P.d.S.); sergio.neves@ime.eb.br (S.N.M.)
* Correspondence: douglas@ime.eb.br

Abstract: Reliable ballistic armor systems are crucial to ensure the safety of humans and vehicles. Typically, these systems are constructed from various materials like fiber-reinforced polymer composites, which are utilized for a favorable weight to ballistic protection ratio. In particular, there has been a quest for eco-friendly materials that offer both strong mechanical properties and sustainable advantages. The present work conducted a ballistic analysis of epoxy matrix composites using raffia (*Raphia vinifera*) fibers from the Amazon region as reinforcement. The experiments investigated the limit and residual velocities of composites with 10, 20, and 30 vol% of raffia. The experimental density of the composites was lower than that of the epoxy. Fractured surfaces were examined by scanning electron microscopy (SEM) to reveal the failure mechanism. The results showed that composites with 10 vol% raffia fiber fabric had the highest ballistic energy absorption (168.91 J) and limit velocity (201.43 m/s). The ones with 30 vol% displayed a higher level of physical integrity. The SEM micrographs demonstrated the failure mechanisms were associated with delamination and fiber breakage. There was a small variation in residual velocity between the composites reinforced with 10, 20, and 30 vol% of raffia, with 826.66, 829.75, and 820.44 m/s, respectively.

Keywords: raffia fiber fabric; *Raphia vinifera*; ballistic behavior; failure mechanisms

1. Introduction

Utilizing renewable and biodegradable materials is one way to enhance the overall quality of life on Earth [1]. Around 2.5 billion tons of lignocellulosic materials, a type of natural resource, are accessible globally and have been utilized as early as 6000 BC [2]. Natural lignocellulosic fibers (NLFs), also known as plant fibers, can be found in a variety of common and technical materials. Brazil stands out among South American countries as a major producer of NLFs, with approximately 8.5 million km^2 of land, of which around 3.5% is urbanized, 30.2% is used for agriculture, and 66.3% is dedicated to protected vegetation [3]. It also benefits from excellent weather and fertile soil, allowing for the growth of a diverse range of plants. This is particularly the case of the Amazon region, with a rich biodiversity comprising a significant number of NLFs.

The utilization of NLFs instead of synthetic fibers in polymer composites has been increasing in various industrial sectors, including packaging, automotive, and construction, over the past few decades [4–6]. This is primarily because of the distinct qualities of NLFs, including their abundance, ability to break down naturally, light weight, nonharmful properties, being gentle on machinery, beneficial mechanical traits, and cost-effectiveness [7,8].

Moreover, NLFs have shown promise in the production of composites for ballistic armor applications. The rise in interpersonal violence, combined with advancements in weapons and ammunition technology, has prompted researchers in ballistic armor to explore new materials that can withstand various threats, aiming to create products suitable

for both civilian and military use. Numerous materials have undergone testing to withstand a wide range of risks [9,10].

One possible solution is to create multilayer armor systems (MASs) that blend the characteristics of various materials. In the front layer, a ceramic material can withstand the impact of the projectile by fragmentivy, absorbing much of the ballistic energy. The residual energy coming from the cloud of projectile and ceramic fragments is taken in by a second layer, which could consist of either polymeric or composite materials. A back layer can be taken into account for final energy absorption and body protection. Generally, aeronautical aluminum and aramid fibers can be utilized for the following layers. As such, the MAS is responsible for absorbing the energy of the projectile and stopping projectile fragments and armor components from penetrating the target from behind [11,12].

At present, advanced synthetic fiber materials like aramid (Kevlar® and Twaron®) and ultra-high-molecular-weight polyethylene (Spectra® and Dyneema®) are being employed in the second layer of armor [13,14]. Nevertheless, these fibers are relatively expensive and not able to be renewed, with a comparatively brief lifespan [8,15].

In this situation, composites with NLFs as reinforcements become a viable alternative for synthetic fiber fabrics in MASs owing to their light weight, affordability, and eco-friendliness [8,15]. NLFs have shown efficient ballistic protection and researchers have shown increasing interest in enhancing their properties for current applications [16,17].

Garcia Filho et al. [18] reported how up to 50 vol% of piassava fibers impacted the value of E_{abs} and limited the velocity of piassava fiber/epoxy composites when tested against 7.62 mm M1 full-metal-jacketed ammunition. The condition with 10 vol% showed the greatest E_{abs} compared to all other conditions tested. Nevertheless, the authors attributed this E_{abs} to the composite's fragmentation mechanism, a consequence of the brittle epoxy matrix. Additionally, the lost integrity state may not be ideal for use in ballistic armor due to the multiple-hit standard requirement.

Neuba et al. [19] reported how up to 30 vol% of *Cyperus malaccensis* sedge fibers impacted the value of E_{abs} and the limit velocity of *Cyperus malaccensis* sedge fiber/epoxy composites when tested against 7.62 mm ammunition. Epoxy composites with a 20 vol% sedge fiber reinforcement showed the highest energy absorption of all tested samples. Composite plates reinforced with 30 vol% sedge fiber have shown appropriate ballistic performance due to the improved E_{abs} and by maintaining a significantly acceptable physical integrity. Nevertheless, the energy absorbed by these materials does not match Twaron and Kevlar™ when used in the same test conditions.

Braga et al. [20] reported how up to 30 vol% of curaua fibers impacted the E_{abs} and the limit velocity of curaua fiber/polyester composites when tested against 7.62 mm ammunition. As per the authors' perspective, the neat polyester resin exhibited the greatest E_{abs}. Nevertheless, its tendency to break into smaller pieces makes it not suitable for multiple impacts. However, the 30 vol% curaua fiber composites exhibited a promising set of features for multiple-impact scenarios, including a high value of E_{abs} and a strong cohesion post-impact.

Braga et al. [21] utilized an up to 30 vol% sisal fiber-reinforced epoxy composite as the middle layer in the MAS. The ballistic performance of the MAS was examined by testing its response to 7.62 mm ammunition. As per the authors, the MAS was not appropriate. Nonetheless, a sisal fiber composite with a volume fraction of 30% as an intermediate layer showed identical ballistic performance to a system based on Kevlar. Using sisal fibers instead of Kevlar in the intermediate layer with epoxy provided a significant economic benefit for the MAS.

Luz et al. [22] investigated how coir fiber-based multilayer armor systems responded to 7.62 mm ammunition with an up to 30 vol% of coir fiber-reinforced epoxy composite. The ballistic performance of the intermediate layer with a 30 vol% of coir fiber was somewhat comparable to that of Kevlar with the same thickness. The authors reported that the coir fiber layer did not hold up against the second impact, resulting in delamination and fiber

pullout as signs of failure. Additionally, unlike Kevlar, utilizing coir fibers in the middle layer with epoxy lowers the cost of the MAS.

Monteiro et al. [23] used sugarcane bagasse to create a ballistic composite. Bagasse is a leftover or waste product created during the process of extracting juice, sugar, and ethanol from sugarcane. The study showed that the bagasse-based composite met the National Institute of Justice (NIJ) test standard [24] for ballistic performance, with clay added as the fourth layer in the MAS.

Demosthenes et al. [25] found that 10 vol% buriti fabric reinforced with epoxy composites did not maintain their integrity and did not meet the NIJ Standard [24] requirements. Cracks were observed in the samples containing 20 vol% buriti fabric, suggesting they also failed to meet the NIJ Standard. On the other hand, the composites containing 30 vol% buriti fabric exhibited some damage from the cloud of fragments at the plate's center, yet did not display any visible failure, in contrast to the composites with 10 and 20 vol%. As stated by the authors, this indicates that 30 vol% buriti fiber composites can be utilized in making bulletproof vests to withstand level III 7.62 mm ammunition.

Among the NLFs, raffia, a fiber derived from the *Raphia vinifera* palm tree leaf, has been commonly used in the Amazon region for a long time. Common uses for its fibers include carpets, ropes, and handicrafts. Recently, Silva et al. [26] performed a thermochemical and structural analysis on a fabric made of raffia fiber and indicated the possibility for the production of polymeric composites for engineering applications.

In the scientific context, this work is justified by the understanding of the mechanical and physical properties of composites reinforced with raffia fabric, and the mechanisms of adhesion and reinforcement between fiber and epoxy matrix. In addition, composite materials with high mechanical performance can be obtained, which can be applied in several sectors in addition to ballistic protection, such as in the automotive, naval, and aerospace industries.

Economically, the use of these fibers is also justified, as they have a low initial cost when compared to synthetic fibers, which are generally imported and have a limited operational lifespan. Therefore, all of these factors contribute to the field of use of NLFs being further expanded, having a scope beyond the classic applications in the textile industry, boosting growth in the agricultural sector, generating jobs for rural communities, and encouraging the production of technologically innovative materials in the country.

Furthermore, the novelty of the work consists in the study of the ballistic behavior of composites with an epoxy matrix reinforced with raffia fabric. The investigation of the properties that occur at the interfaces of the components of the armor systems also emerges as an original contribution of this work to the state of the art, both in the field of polymer composites reinforced with NLFs and in ballistic armor.

Therefore, the present work aims to investigate the ballistic performance of epoxy matrix composites reinforced with up to 30 vol% of fabrics made from raffia fiber. Standalone ballistics tests using 7.62 mm caliber projectiles allowed us to evaluate the absorbed impact energy and the limit velocity withstood by the composite target. Analysis of variance (ANOVA) and Tukey's test provided statistical validation for the ballistic results. Fracture mechanisms were identified by scanning electron microscopy (SEM).

2. Materials and Methods

2.1. Materials

A Bisphenol A diglycidyl ether (DGEBA) epoxy resin was utilized as the matrix phase, mixed with a hardener containing triethylenetetramine (TETA) in a 100:13 stoichiometric ratio. It was considered that the epoxy resin had a density of 1.11 g/cm^3 based on other studies [27]. Dow Chemical (São Paulo, Brazil) created these materials, which Resin Epoxy Ltd. (Rio de Janeiro, Brazil) distributed.

Raffia fibers from *Raphia vinifera* species were bought in the city of Belém (Brazil) as flat-woven fabrics, as shown in Figure 1. The calculated raffia fiber density was indicated to have a value of 0.95 g/cm^3 [26].
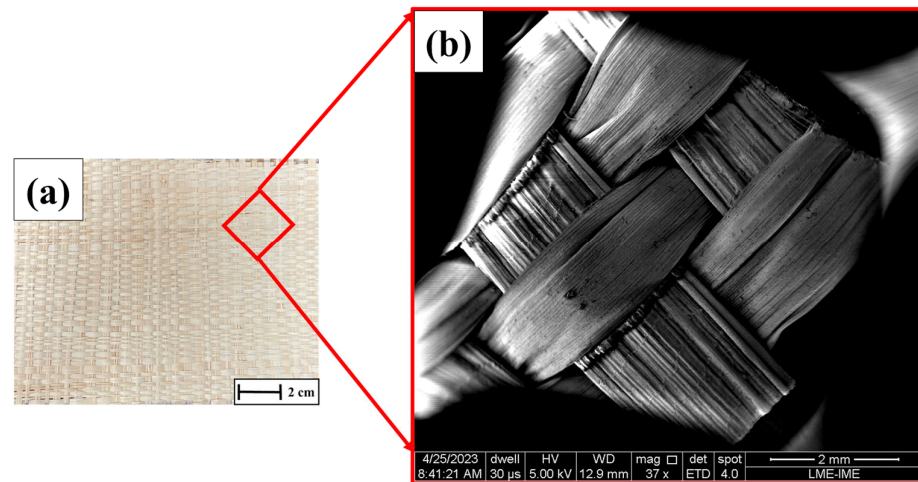
Figure 1. (**a**) Fabric made from extracted fibers; (**b**) Weft in an SEM micrograph with $37\times$ magnification.

2.2. Methods

2.2.1. Composite Manufacturing

The as-received raffia fabric was sliced into rectangles measuring 120×150 mm and placed in an oven at 60 °C for 24 h to remove any moisture. The fabrics were carefully arranged in a metallic mold to create plates with dimensions measuring $150 \times 120 \times 12$ mm. The mold metallic surfaces were coated with silicone grease to avoid friction during the removal of the composite plate. The raffia fabrics were carefully positioned in the mold and soaked with the resin and hardener. After closing the mold, a pressure of 5 tons was applied for 24 h. Plates containing 10, 20, and 30 vol% of raffia fibers were manufactured after the curing process, as shown in Figure 2, conducted at room temperature (RT~25 °C).
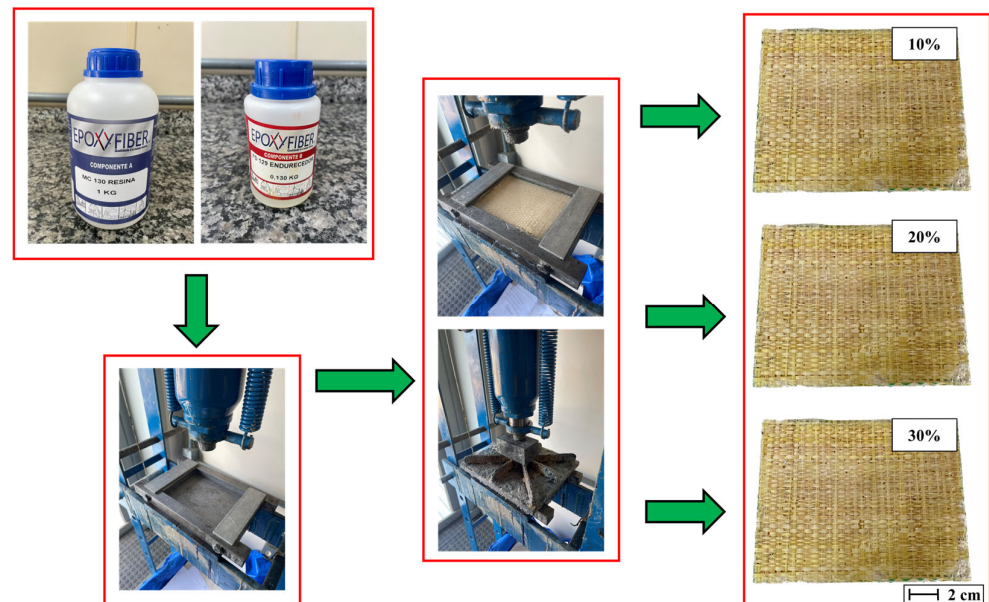
Figure 2. Depiction of the production process of the raffia fiber fabric board.

2.2.2. Density Determination of Composites

The experimental density was performed on the composites measuring 25×25 mm using the Archimedean principle. The composite, after curing, was subsequently weighed in air and then weighed again in a liquid of a known density. Five samples from each

condition were tested. The density was calculated based on the measured values, noted in g/cm^3, according to the following:

$$E_D = \frac{(M_s \times \rho_L)}{(M_U - M_I)} (g/cm^3)$$

(1)

where M_S is the dry mass (g), M_U is the naturally wet mass (g), M_I is the liquid-immersed mass (g), and ρ_L is the specific mass of water (g/cm^3).

The theoretical density was calculated according to the rule of mixtures as follows:

$$T_D = \frac{100}{\frac{R}{D} + \frac{r}{d}} (g/cm^3)$$

(2)

where R represents the percentage of resin by weight, r denotes the percentage of raffia fabric by weight, the density of resin is represented by D in g/cm^3, while the density of raffia fabric is represented by d in g/cm^3.

2.2.3. Stand-Alone Ballistics Tests

Ballistics tests were performed at the Brazilian Army Assessment Center (CAEx) in Rio de Janeiro, Brazil, as illustrated in Figure 3. Six shots were fired in each tested condition. The High-Pressure Instrumentation (HPI) gun barrel, as shown in Figure 3a, was positioned at a distance of 15 m from the target sample, as shown in Figure 3b. A B290 with a laser sight to the sample, as shown in Figure 3c, was utilized as the shooting apparatus. Commercial 9.7 g, 7.62 mm M1 full-metal-jacketed ammunition, as shown in Figure 3d, was utilized. The direction exhibited by the bullet was identified as perpendicular to the target. To determine the speed of the projectile pre- and post-impact, an SL-520 P Weibel Doppler radar, Denmark, was used along with Windopp software for the data analysis.
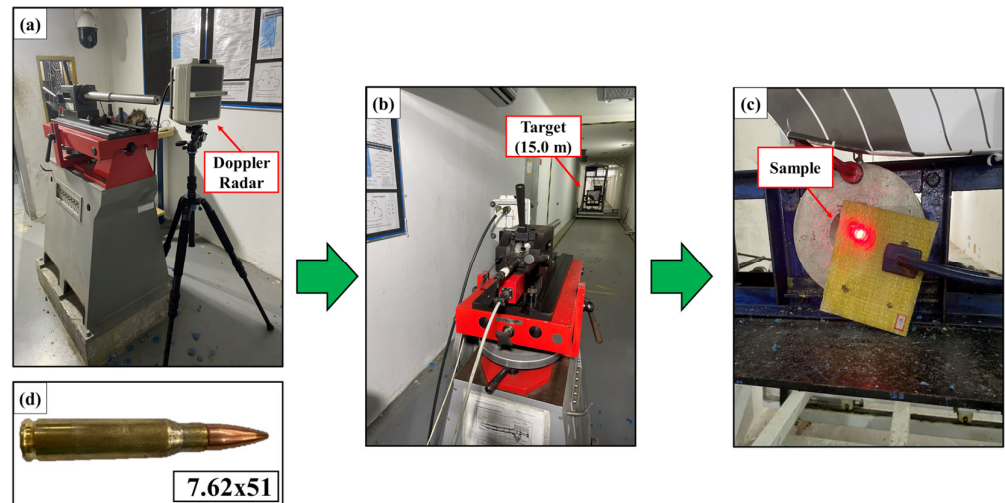
Figure 3. (**a**) High-Pressure Instrumentation (HPI) weapon and Doppler radar; (**b**) Distance of 15 m from the target sample; (**c**) Sample positioned with laser sight; (**d**) Commercial 9.7 g, 7.62 mm M1 full-metal-jacket ammunition.

As previously stated, the projectile's achieved velocities were determined both pre- (V_i) and post-hitting (V_r) the target. The difference in kinetic energy was linked to the amount of energy absorbed (E_{abs}) by the target according to the following:

$$E_{abs} = \frac{m_p (V_i^2 - V_r^2)}{2}$$

(3)

where m_p is the mass of the projectile. Additionally, the limit velocity (V_L) is another crucial dynamic parameter in ballistic armor, according to Equation (4). V_L is the velocity at which

the ammunition can be stopped by the target and can be estimated. When V_r is set to zero, it is as follows:

$$V_L = \sqrt{\frac{2E_{abs}}{m_p}} \tag{4}$$

The radar captured the data which allowed to show a frequency spectrum over time, which could be analyzed using Fast Fourier Transform (FFT) to determine the correlation between the intensity and the velocity curve fitting, as shown in Figure 4. This figure displays the data points from an experiment using a composite sample containing 30 vol% raffia fabric, as well as the curve obtained from adjusting a continuous polynomial relationship. Furthermore, it is important to mention that there is a sudden decrease at 868 m/s, showing the velocity at the moment of impact. Following this, the velocity drops to 859 m/s, demonstrating the residual velocity after the target penetration.
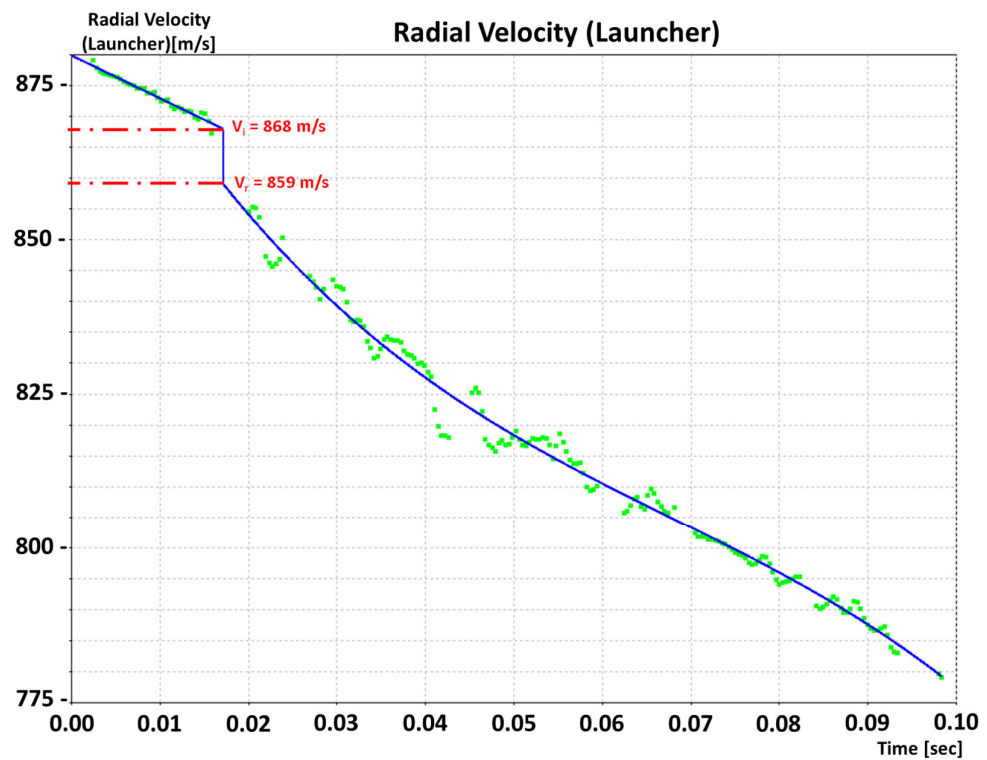
Figure 4. Data from radar spectrum and FFT curve-fitting experimental points.

2.2.4. Statistical Analysis

Through ANOVA analysis, statistical treatment was applied to the results of the ballistics tests for a confidence level exceeding 95%. It also offered an assessment on whether the amount of fiber added as reinforcement in the composites affected the obtained outcomes. Tukey's test compared the average values to determine if there was a notable difference between the distinct conditions being tested. This was alternatively referred to as honestly significant difference (HSD), expressed according to the following:

$$HSD = q\sqrt{\frac{EMS}{r}} \tag{5}$$

where q represents the *HSD* constant tabulated for a significance level of 5%, *EMS* stands for the error mean square in the ANOVA, and r represents the number of times each treatment was repeated.

2.2.5. Fracture Surface Analysis

The examination of the primary mechanisms of failure associated with the fracture was conducted following the ballistics testing of the composite plates on both macro- and microscopic scales. The fractured samples were analyzed by SEM in a Quanta FEG 250 FEI model (Thermo fisher Scientific, Waltham, MA, USA) functioning with secondary electrons at 10 kV.

3. Results and Discussion

3.1. Density Analysis

Table 1 shows the values obtained for the dry mass, wet mass, and liquid-immersed mass for each tested condition, and Table 2 and Figure 5 show the density results for the composites according to Equations (1) and (2).

Table 1. Values obtained for the dry mass, wet mass, and liquid-immersed mass for the composites.

| | **Conditions** | | | | | | | | |
| | **10%** | | | **20%** | | | **30%** | | |
	MS [a] (g)	**MU [b] (g)**	**MI [c] (g)**	**MS [a] (g)**	**MU [b] (g)**	**MI [c] (g)**	**MS [a] (g)**	**MU [b] (g)**	**MI [c] (g)**
	3.37	3.58	0.37	5.82	6.18	0.38	2.09	2.32	0.09
	3.58	3.78	0.33	2.97	3.14	0.17	2.42	2.72	0.14
	2.91	3.15	0.23	3.08	3.32	0.25	2.21	2.49	0.12
	3.23	3.53	0.37	2.48	2.78	0.19	3.06	3.28	0.17
	4.29	4.81	0.53	2.60	2.84	0.16	2.82	3.09	0.17
M [d]	3.48	3.78	0.37	3.39	3.66	0.23	2.52	2.78	0.14
SD [e]	0.52	0.63	0.11	1.38	1.43	0.09	0.41	0.40	0.03

[a] Dry mass; [b] Wet mass; [c] Liquid-immersed mass; [d] Mean; [e] Standard deviation.

Table 2. Experimental and theoretical density of the composites compared to the plain epoxy.

Sample	E.D [a] (g/cm^3)	T.D [b] (g/cm^3)	Reference
10 vol% raffia fabric	0.55 ($\pm$0.12)	1.08	PW*
20 vol% raffia fabric	0.69 ($\pm$0.08)	1.06	PW*
30 vol% raffia fabric	0.76 ($\pm$0.02)	1.05	PW*
Plain epoxy	1.11	-	[28]

PW*—Present work; [a] E.D—Experimental density; [b] T.D—Theoretical density based on the rule of mixtures.

Indeed, the addition of 10, 20, and 30 vol% of raffia fabric caused a decrease in the density in relation to the plain epoxy. This decrease in composite densities might be attributed to the great hygroscopicity of the raffia fabric. Natural raffia fiber has a lower density compared to epoxy. Consequently, increasing the fiber content should decrease the overall density of the composite. By contrast, the results obtained for the theoretical densities based on the rule of mixtures was the opposite compared with the experimental densities. This comparison helped us to identify a discrepancy arising from the experimental conditions with 96.32%, 53.62%, and 38.15% for the addition of 10, 20, and 30 vol% of raffia fabric, respectively.

According to Swain and Biswas [29], the density of a composite material is determined by the ratio of reinforcing and matrix materials, which plays a crucial role in determining the properties of the composites. The discrepancy in the calculated density versus the experimental density is due to the presence of void content. The presence of void spaces significantly impacts certain mechanical characteristics and can hinder the performance of composites in industrial settings. Having fewer voids is expected in a high-quality composite. The existence of void spaces cannot be avoided when creating composites, especially when using the hand-lay-up method.
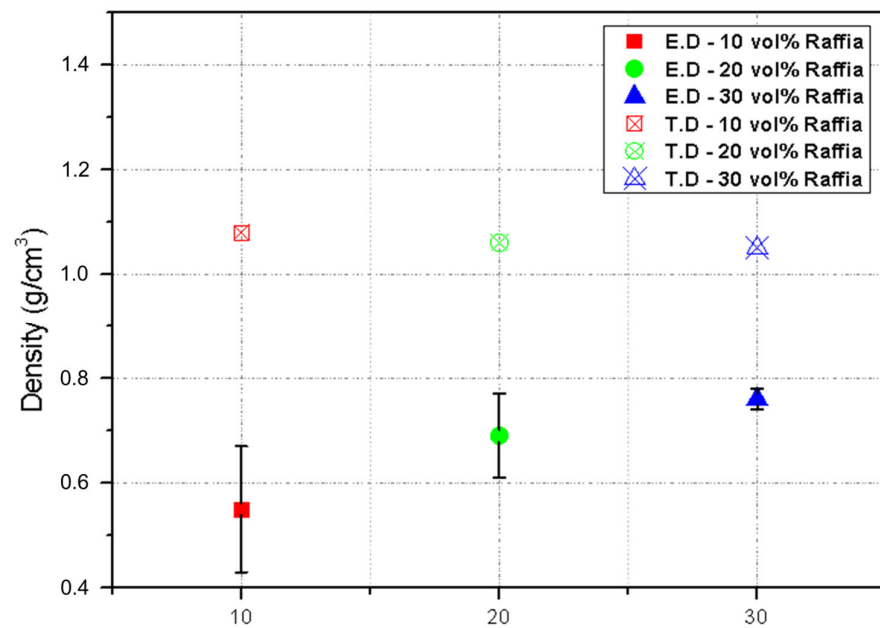
Figure 5. Comparison of experimental and theoretical densities under various conditions of composite plates.

The primary attributes of voids in fiber-reinforced composites (FRCs) include the void content, shape, size, location, and distribution. These traits may vary greatly, even within various parts of the same sample. Material properties and processing parameters impact the void content and distribution within a particular FRC. These factors include polymer rheology, the wettability of fibers by polymer, and volatile components in the polymer, as well as temperature, pressure, and time [30]. Different material systems and process types can exhibit varied void shapes, sizes, and positions [31].

Unwanted void spaces usually develop in polymers due to the trapping of air during the liquid processing. Unwanted voids can also form in a thermoset polymer resin while it cures because of the gas produced by chemical reactions between the resin and catalyst [32]. The presence of non-uniformity at a microstructural scale has caused challenges in studying the movement of moisture. When polymers with void spaces come into contact with water, the water molecules penetrate the resin until they reach the edge of the void space. He and Fan [33] propose that moisture absorbed into voids must condense in order to create liquid water.

The impact of void spaces on the absorption of water by composite materials containing a polymer matrix has been examined. Thomason [34] researched the absorption of moisture in glass/epoxy composites at high relative humidity levels and discovered that voids significantly increase the moisture absorption. He discovered that composites with void spaces soaked up a significantly higher amount of water compared to the resin part.

The amount of water absorbed by the composite depends on many factors, ranging from the type of polymeric matrix used, the surface treatment of the NLF, the microcavities present in the fiber, to the hydrophilic nature of the fiber. In the case of the relief of the fiber surface, the microcavities may undergo changes due to occasional interactions with the polymer matrix. Generally speaking, the greater the interaction between the fiber and the matrix, the smaller the number of voids available, which can, for example, be used to accommodate or store water [35].

Additionally, vegetable fibers, as they have two very distinct regions made up of lignin and cellulose, have different interactions with water. The regions of the plant fiber composed predominantly of lignin can assimilate or accommodate more water due to their amorphous structure, while the crystalline and, consequently, more compact structure of cellulose presents greater restrictions on the accommodation of moisture. The hydration

property of the fiber, that is, the fiber's ability to absorb water, can be defined by the amount of water bound to the fiber without any application of external force, other than gravitational force and atmospheric pressure. The hydration property will basically depend on three main factors, the fiber's ability to bind with water, its ability to retain water, and the fiber's swelling capacity (storage space). The main factor in promoting the bonding of water with the fiber is the chemical group OH, which can form chemical bonds with it [35].

The moisture-absorbing properties of NLFs affect the material's biodegradation properties. Additionally, increased moisture absorption allows for increased microbial attack. These occurrences impact the bonding between the fiber and matrix at the interface, resulting in ineffective stress transfer and altering the physical, mechanical, and thermal characteristics of the composite [36,37].

Moreover, it is important to note that the composites have a distinct advantage in terms of density, given that natural fibers are lighter and less dense when compared to synthetic fibers [38]. In addition to low density, the raffia, as NLFs, possess an inner space, known as the lumen, which can change shape, resulting in significant fluctuations in diameter throughout their length. This leads to a reduction in the fiber density, which boosts the acoustic and thermal insulation abilities while also impacting the fiber tensile strength [39].

3.2. Stand-Alone Ballistics Test Results

In the ballistic experiments, the values of V_i and V_r were calculated using Equation (3), enabling the computation of E_{abs}. Tables 3 and 4 and Figure 6 display the results found in the ballistic tests of the composite samples for each group condition.

Table 3. The outcomes of energy absorption under various conditions of the composite plates.

Conditions	10%	20%	30%
	206.96	108.34	181.08
	197.33	93.83	160.78
	205.09	105.79	164.00
Energy absorbed (J)	206.81	97.87	198.85
	198.83	79.73	182.46
	167.24	81.42	170.47
Mean	168.91	81.03	151.13
Standard deviation	13.84	10.95	12.88

Table 4. Limit, residual, and impact velocities for the composite plates reinforced with raffia fabric tested.

		Conditions							
		10%			20%			30%	
	V_i (m/s)	V_r (m/s)	V_L (m/s)	V_i (m/s)	V_r (m/s)	V_L (m/s)	V_i (m/s)	V_r (m/s)	V_L (m/s)
	872.40	847.59	206.57	842.73	829.37	149.46	833.04	810.32	193.23
	840.92	816.37	201.71	843.34	831.79	139.09	831.44	811.26	182.07
	833.98	808.23	205.64	844.55	831.61	147.27	845.05	824.80	183.89
	845.63	820.03	206.49	833.12	820.92	142.05	840.33	815.57	202.48
	835.32	810.41	202.47	842.80	832.99	128.22	838.92	816.19	193.96
	877.23	857.35	185.69	841.84	831.81	129.56	865.05	844.49	187.48
M [a]	850.91	826.66	201.43	841.39	829.75	139.28	842.30	820.44	190.52
SD [b]	17.37	18.85	7.29	3.79	4.09	8.08	11.14	11.73	6.91

[a] Mean; [b] Standard deviation.
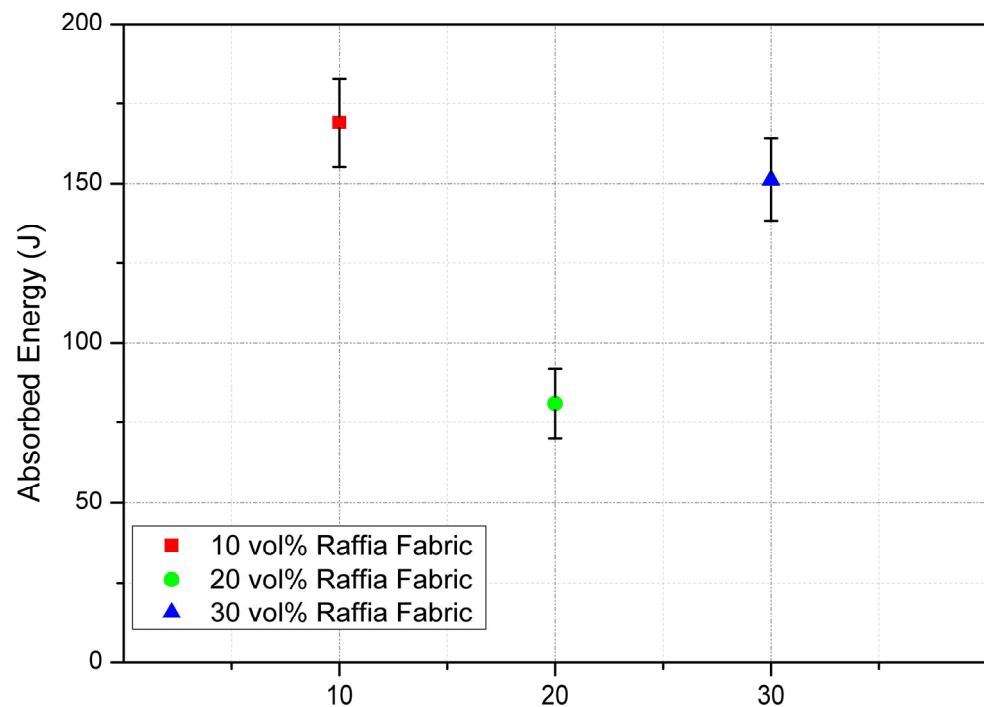
Figure 6. Comparison of energy absorption under various conditions of composite plates.

The results show that the plates made from 10 vol% raffia fabric had the highest E_{abs} of 168.91 J and a limit velocity of 201.43 m/s; the plates made from 30 vol% raffia fabric had the second highest value of E_{abs} of 151.13 J and a limit velocity of 190.52 m/s; the plates made with 20 vol% raffia fabric had the lowest value of E_{abs} of 81.03 J and a limit velocity of 139.28 m/s.

The greatest E_{abs} occurs at a 10 vol% fiber content, with the lowest absorption at 20 vol%, and none at 30 vol%. Among the defects that may arise from manufacturing, it is worth mentioning regions rich in resin or fiber, distorted or bent fibers, and the presence of contaminants and voids, with the latter being of great concern, as they are difficult to avoid and considerably impair the performance of the composite [40]. The formation of voids in composites is generally due to the presence of air bubbles trapped between the fiber reinforcement bundles, moisture absorbed by the reinforcement during storage, inadequate process parameters, such as time, pressure, and temperature, and/or originating from the resin when formulated [41,42]. These conditions might also justify the experimental decrease in the composite's densities shown in Table 2.

The creation of void spaces within the composites will diminish the mechanical characteristics of the composites [42,43]. The occurrence of void spaces in polymer composites is primarily attributed to leftover solvents, volatile substances emitted during the curing of resin, and the trapping of air during the mixing of resin [44]. Moreover, the rise in gaps with the addition of raffia fabric as reinforcement was caused by the trapped moisture in the fibers resulting from the hydroxy group presence in hemicellulose and cellulose, which have a tendency to attract water molecules [45].

Despite the excellent properties and advantages in terms of use, NLFs also have some disadvantages when used in polymer composites, such as being microstructurally and dimensionally heterogeneous, as well as having a great affinity for humidity. Not to mention that a species of fiber may have its properties affected depending on the origin, plant quality, plant age, fiber diameter and aspect ratio, and its preconditioning [46].

The ability of epoxy composites reinforced with raffia fabric to withstand 7.62 mm caliber ammunition is similar to that of other composites reinforced with NLFs [18–24]. Table 5 shows a comparison of the ballistic resistance of different composites reinforced

with NLFs in a 7.62 mm ammunition test, as well as previously reported results for plain epoxy and Kevlar^{TM}.

Table 5. Comparison of the ballistic resistance of different composites reinforced with NLFs in a 7.62 mm ammunition test, as well as previously reported results for plain epoxy and Kevlar^{TM}.

Sample	E_{abs} (J)	V_L (m/s)	Reference
10 vol% raffia fabric	168.91	201.43	PW*
20 vol% raffia fabric	81.03	139.28	PW*
30 vol% raffia fabric	151.13	190.52	PW*
10 vol% ubim fibers	187.03	195.98	[47]
20 vol% ubim fibers	169.07	185.98	[47]
30 vol% ubim fibers	159.42	180.79	[47]
10 vol% TVFs**	171.82	192.06	[48]
20 vol% TVFs**	176.19	193.88	[48]
30 vol% TVFs**	166.51	188.84	[48]
DGEBA/TETA epoxy	190.00	196.00	[49]
Kevlar (ply of aramid fabric)	58.00	109.00	[50]

PW*—Present work; TVFs**—Titica vine fibers.

When the experimental data are compared to the results from other studies conducted under similar conditions, it is evident that raffia fabric-reinforced composites exhibit ballistic performance on par with various other reinforced composites. In particular, the composite with 10 vol% raffia fabric achieved similar ballistic performance as epoxy matrix composites reinforced with ubim fibers [47] and titica vine fibers [48].

Previously, it was discovered that a plain epoxy has a high limit velocity (196 m/s) but will break completely when hit by a 7.62 mm projectile [49]. Compared to that, a Kevlar^{TM} plate by itself remained intact, and its limit velocity was 109 m/s [50]. Once more, the preservation of the physical structure of the materials needs to be taken into account. The plain epoxy exhibited higher E_{abs} values, but also either completely cracked or developed long cracks, which compromised their structural integrity.

3.3. Statistical Analysis

3.3.1. Statistical Analysis of Experimental Density

An ANOVA analysis was conducted, and the parameters, according to Table 6, indicate its reliability. It was confirmed that F was higher than Fc, since the values of F and Fc were, respectively, 7.32 and 3.89. Therefore, it can be inferred that the mean values are the same when the hypothesis is rejected with a certainty level equal to 95%. The varying quantities of fibers in the composites had an impact on the experimental density, as evidenced by the statistical results.

Table 6. Performing an ANOVA analysis to acquire the experimental density outcomes.

Causes of Variation	Degrees of Freedom	Sums of Squares	Mean Square	F (Calculated)	Fc (Tabulated)
Treatment	2	0.111	0.055	7.32	3.89
Residue	12	0.091	0.007		
Total	14	0.202			

Tukey's test, shown in Table 7, was used to obtain a comparison of experimental density mean values. The value of 0.12 g/cm³ for the HSD was acquired using Equation (5). It was observed that only the composite groups of 20 and 30% did not show a significant difference. Furthermore, it could be concluded that there is, in fact, an increasing trend between the groups of 10 and 30%.

Table 7. Average values of the Tukey test for density through composite plates.

Conditions	10%	20%	30%
10%	0	0.137	0.207
20%	0.137	0	0.070
30%	0.207	0.070	0

3.3.2. Statistical Analysis of Energy Absorption

An ANOVA was conducted. The statistical parameters in the ANOVA analysis impacted its reliability, as indicated in Table 8. It was confirmed that F was larger than Fc, as the value of F was 11.39 compared to the value of Fc of 3.89. Therefore, it can be inferred that the average values are the same when the hypothesis is rejected with a 95% certainty. The varying quantities of fibers in the composites had an impact on the E_{abs}, as evidenced by the ANOVA results.

Table 8. Performing an ANOVA analysis to acquire the energy absorption outcomes.

Causes of Variation	Degrees of Freedom	Sums of Squares	Mean Square	F (Calculated)	Fc (Tabulated)
Treatment	2	17,535.49	8767.74	11.39	3.89
Residue	12	9235.98	769.66		
Total	14	26,771.47			

Additionally, the Tukey test, shown in Table 9, was used to link the average values. The value of 37.89 J for the HSD was determined through the use of Equation (5). Table 9 depicts the correlation between the average values comparing the HSD. The highlighted differences in the average values were greater than the HSD, and can be seen in this table.

Table 9. Average values of the Tukey test for absorption through the composite plates.

Conditions	10%	20%	30%
10%	0	83.50	36.18
20%	83.50	0	47.32
30%	36.18	47.32	0

3.4. Fracture Surface Analysis

The structural soundness of the composite plates (CPs) is another crucial aspect to take into account when using materials for ballistic armor. In the tests on residual velocity using 7.62 mm ammunition, all of the projectiles pierced through every sample. The tested samples are displayed in Figures 7–9.
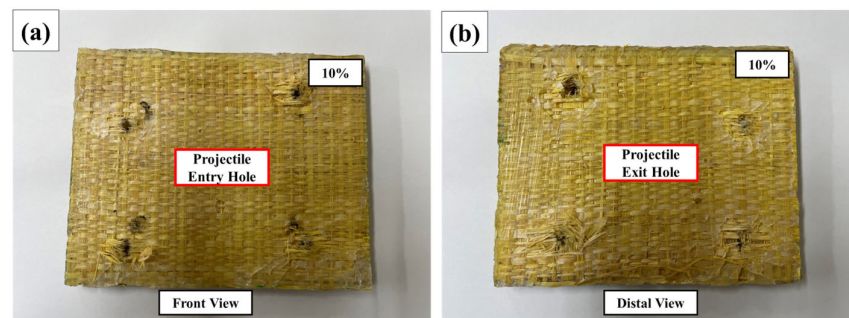
Figure 7. Appearance of the composite material target after the ballistic impact for raffia fabric-reinforced epoxy composites with a 10 vol%. (**a**) Front view and (**b**) distal view.
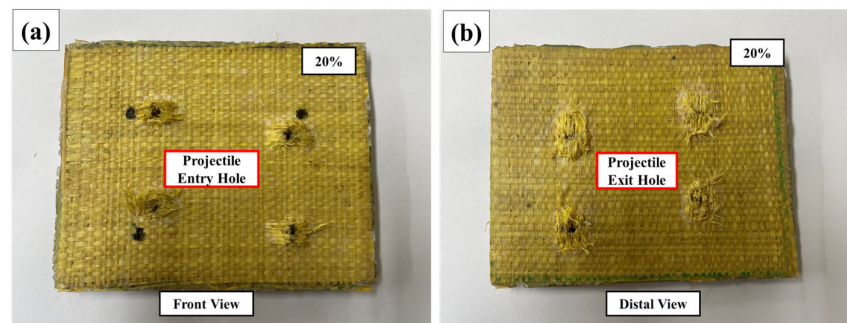
Figure 8. Appearance of the composite material target after the ballistic impact for raffia fabric-reinforced epoxy composites with a 20 vol%. (**a**) Front view and (**b**) distal view.
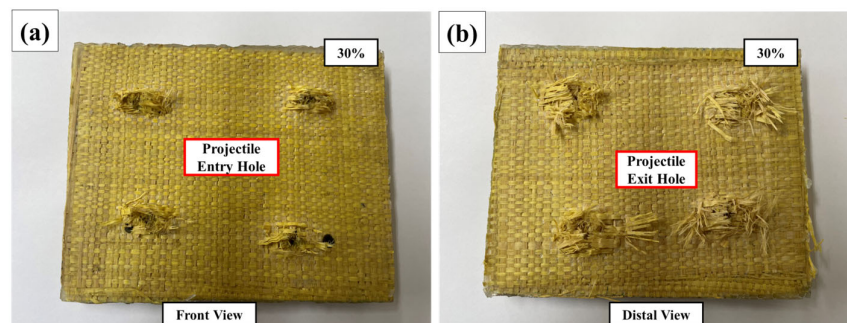
Figure 9. Appearance of the composite material target after the ballistic impact for raffia fabric-reinforced epoxy composites with a 30 vol%. (**a**) Front view and (**b**) distal view.

The figures show how the specimens look following the residual velocity test. It is clearly shown in the pictures that the raffia fabric effectively helped prevent the spread of fissures and cracks, thereby preserving the material's integrity. However, it was not effective in increasing the E_{abs}. Indeed, the materials used for ballistic shielding should remain intact after the initial shot, and should be able to endure multiple impacts while still absorbing a relatively higher amount of ballistic energy.

The samples containing 30 vol% raffia fabric showed superior physical integrity compared to the other samples, but had a lower post-impact E_{abs}. Some previous studies have emphasized the significance of maintaining physical integrity in the test specimens of materials for personal ballistic armor [47,50]. Another significant factor that encourages the utilization of the 30 vol% raffia fabric is the correlation between the amount of raffia fabric utilized and the decrease in the price of the composite.

In addition to enhancing the performance and prioritizing environmental concerns, the economic and weight evaluation of using NLFs instead of synthetic ones, particularly in ballistic composites, is highly important. A decreased price encourages the replacement of synthetic fiber by NLFs in numerous past research studies. In their study, Monteiro et al. [50] achieved a cost reduction of 31.2% by substituting aramid fiber for natural curaua fiber in an MAS. The study conducted by Braga et al. [21] assessed the cost and weight implications of substituting aramid with sisal fiber in a multilayered armor composite. The analysis findings showed a 275% decrease in cost as a result of the replacement.

According to Odesanya et al. [51], the prices of synthetic fibers fluctuate over time, but particularly decrease when the prices of oil products drop. This decrease in price is expected to grow along with advancements in technology. But, as per the authors' perspective, the main purpose of analyzing these fibers economically is to help researchers choose the most cost-effective, lightweight, and environmentally friendly NLF for ballistic applications without compromising their effectiveness.

SEM was used to capture micrographs for a more thorough assessment of the fracture mechanisms. These micrographs facilitated the identification of fracture mechanisms in

both the fibers and the matrix. Figures 10–12 show the SEM images for the composites that include 10 to 30 vol% raffia fabric.
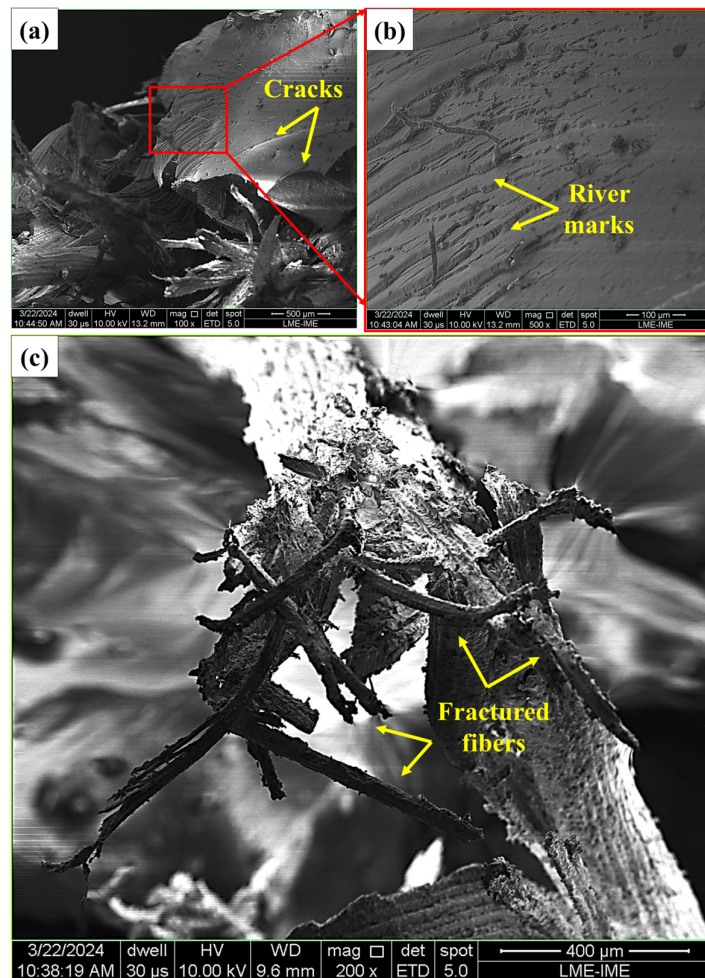
Figure 10. SEM micrographs of the epoxy composite with 10 vol% raffia fabric. (**a**) 100×, (**b**) 500×, and (**c**) 200×.
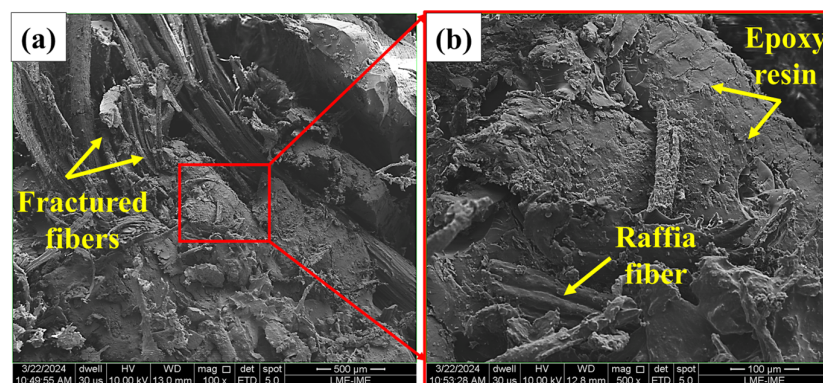
Figure 11. SEM micrographs of the epoxy composite with 20 vol% raffia fabric. (**a**) 100× and (**b**) 500×.
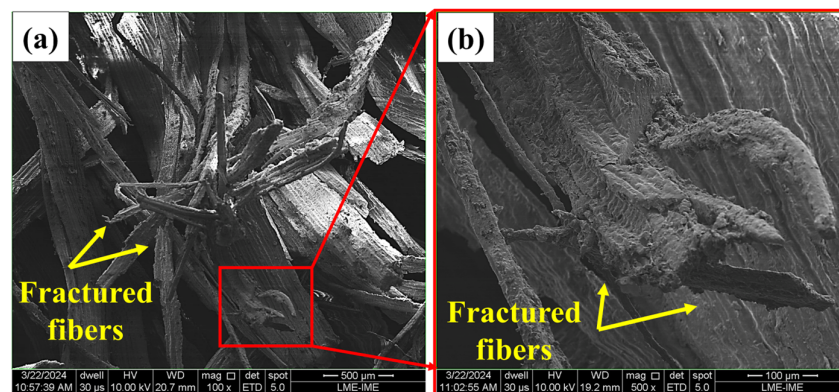
Figure 12. SEM micrographs of the epoxy composite with 30 vol% raffia fabric. (**a**) 100× and (**b**) 500×.

Figure 10a–c show the composite with 10 vol% raffia fabric and highlights multiple active failure mechanisms. The fracture surface displays cracks and fractured fibers with interfaces, revealing the poor bonding between the raffia fiber and the epoxy matrix. Furthermore, the existence of river marks in the material is also clear, and linked to a common type of failure that happens in NLFs/polymer resins in an area with a greater resin content [52].

The composites containing 10 vol% raffia fabric displayed higher E_{abs} values than the other composites. The reason for this could be the heightened activity of the epoxy resin brittle fracture mechanisms, as indicated by the prominent river marks. As river marks are linked to numerous surface fractures post-collision, they tend to absorb a greater amount of energy. The reinforcement phase absorbed the kinetic energy, as shown by the appearance of fiber ruptures and cracks on the material surface. A similar behavior was found by de Assis et al. [53].

Figure 11a,b show fracture surfaces that expose multiple failure mechanisms, such as river marks, delamination, broken fibers, cracks, fibril separation, and matrix fracture. Figure 12a,b also demonstrate consistent failure mechanisms, including fiber breakage and matrix fracture, observed in composites containing 10 and 20 vol% raffia fabric. Nonetheless, the samples containing the 30 vol% raffia fabric showed improved dimensional stability following ballistic impact in comparison to the earlier samples. Even though, with respect to the E_{abs} value, it ranked second, the fibers' performance was easily seen in the micrographs.

Guaruman fibers [12], as well as curaua fibers [54], have demonstrated comparable results during testing for resistance against ballistic impact. The improved adhesion between the fibers and the matrix reduced the amount of energy absorbed by delamination and fiber breaking.

4. Summary and Conclusions

In this study, composites with varying contents of raffia fabric were tested for the first time using 7.62 mm ammunition. Scanning electron microscopy (SEM) was used to analyze the surfaces of the broken samples. The following conclusions are drawn:

- Adding 10, 20, and 30 vol% of raffia fabric to the epoxy resulted a decrease in density in relation to the plain epoxy. This decrease in composite densities might be attributed to the great hygroscopicity of the raffia fabric.
- The comparison of the theoretical densities calculated using the rule of mixtures with experimental densities revealed discrepancies of 96.32%, 53.62%, and 38.15% for the incorporation of 10, 20, and 30 vol% of raffia, respectively. The discrepancy in calculated density versus experimental density can be attributed to the presence of voids.
- The E_{abs} results presented indicated a low degree of compatibilization of the components of the manufactured composites. One way to improve the material characteristics

- can be achieved by using another manufacturing process (vacuum-assisted manual lamination or vacuum infusion) and performing a surface pre-treatment of the fiber.

- Epoxy matrix composites containing 10 vol% raffia fabric showed the highest energy absorption value among the samples tested. The reason for this was mainly due to the fragile nature of the epoxy matrix, leading to the composite plates breaking apart completely. Hence, the lack of integrity post-ballistic impact is considered unsuitable for use in multilayer armor systems (MASs) requiring multiple shots for proper evaluation.

- The 30 vol% raffia fabric composites showed an appropriate ballistic performance by combining improved E_{abs} with good physical integrity. These findings highlight the significance of incorporating NLFs for strengthening polymeric composites and contribute to our understanding, particularly in the case of raffia fabric, which has not yet been documented in the literature.

- SEM micrographs revealed that the epoxy matrix exhibited a brittle fracture mechanism, along with the presence of raffia fiber ruptures, pullout, and delamination on the fractured surface.

- Finally, the current epoxy composites strengthened by raffia fabric were assessed as highly suitable for personal ballistic protection in an MAS, particularly in the role of an intermediate layer. Cost-effectiveness and reduced weight are key factors in the decision to choose this innovative ballistic material.

Author Contributions: Conceptualization, D.S.S.; formal analysis, D.S.S. and R.F.P.J.; investigation, D.S.S. and R.F.P.J.; methodology, D.S.S.; writing—review and editing, M.H.P.d.S. and S.N.M.; supervision, M.H.P.d.S. and S.N.M.; resources, S.N.M.; funding acquisition, S.N.M. All authors have read and agreed to the published version of the manuscript.

Data Availability Statement: The original contributions presented in the study are included in the article, further inquiries can be directed to the corresponding author.

Conflicts of Interest: The authors declare no conflicts of interests.

References

1. Tian, W.; Wang, X.; Ye, Y.; Wu, W.; Wang, Y.; Jiang, S.; Wang, J.; Han, X. Recent progress of biomass in conventional wood adhesives: A review. *Green Chem.* **2023**, *25*, 10304–10337. [CrossRef]
2. Govil, T.; Wang, J.; Samanta, D.; David, A.; Tripathi, A.; Rauniyar, S.; Salem, D.R.; Sani, R.K. Lignocellulosic Feedstock: A Review of a Sustainable Platform for Cleaner Production of Nature's Plastics. *J. Clean. Prod.* **2020**, *270*, 122521. [CrossRef]
3. EMBRAPA. Agriculture and Environmental Preservation Summary of Land Occupation and Use in Brazil. 2018. Available online: https://www.embrapa.br/car/sintese (accessed on 12 May 2024).
4. Ribeiro, M.M.; Pinheiro, M.A.; Rodrigues, J.d.S.; Ramos, R.P.B.; Corrêa, A.d.C.; Monteiro, S.N.; da Silva, A.C.R.; Candido, V.S. Comparison of Young's Modulus of Continuous and Aligned Lignocellulosic Jute and Mallow Fibers Reinforced Polyester Composites Determined Both Experimentally and from Theoretical Prediction Models. *Polymers* **2022**, *14*, 401. [CrossRef] [PubMed]
5. Chandgude, S.; Salunkhe, S. In state of art: Mechanical behavior of natural fiber-based hybrid polymeric composites for application of automobile components. *Polym. Compos.* **2021**, *42*, 2678–2703. [CrossRef]
6. Choi, H.; Choi, Y.C. Setting Characteristics of Natural Cellulose Fiber Reinforced Cement Composite. *Constr. Build. Mater.* **2021**, *271*, 121910. [CrossRef]
7. Rajeshkumar, G.; Seshadri, S.A.; Ramakrishnan, S.; Sanjay, M.R.; Siengchin, S.; Nagaraja, K.C. A comprehensive review on natural fiber/nano-clay reinforced hybrid polymeric composites: Materials and technologies. *Polym. Compos.* **2021**, *42*, 3687–3701. [CrossRef]
8. Zhang, Z.; Cai, S.; Li, Y.; Wang, Z.; Long, Y.; Yu, T.; Shen, Y. High Performances of Plant Fiber Reinforced Composites—A New Insight from Hierarchical Microstructures. *Compos. Sci. Technol.* **2020**, *194*, 108151. [CrossRef]

9. Setlak, L.; Kowalik, R.; Lusiak, T. Practical Use of Composite Materials Used in Military Aircraft. *Materials* **2021**, *14*, 4812. [CrossRef]

10. Key, C.T.; Alexander, C.S. Numerical and Experimental Evaluations of a Glass-Epoxy Composite Material under High Velocity Oblique Impacts. *Int. J. Impact Eng.* **2020**, *137*, 103443. [CrossRef]

11. Meliande, N.M.; Oliveira, M.S.; Pereira, A.C.; Balbino, F.D.P.; Figueiredo, A.B.S.; Monteiro, S.N.; Nascimento, L.F.C. Ballistic properties of curaua-aramid laminated hybrid composites for military helmet. *J. Mater. Res. Technol.* **2023**, *25*, 3943–3956. [CrossRef]

12. Reis, R.H.M.; Nunes, L.F.; da Luz, F.S.; Candido, V.S.; da Silva, A.C.R.; Monteiro, S.N. Ballistic Performance of Guaruman Fiber Composites in Multilayered Armor System and as Single Target. *Polymers* **2021**, *13*, 1203. [CrossRef] [PubMed]

13. Nascimento, R.F.; Silva, A.O.d.; Weber, R.P.; Monteiro, S.N. Influence of UV radiation and moisten associated with natural weathering on the ballistic performance of aramid fabric armor. *J. Mater. Res. Technol.* **2020**, *9*, 10334–10345. [CrossRef]

14. Scazzosi, R.; de Souza, S.D.B.; Amico, S.C.; Giglio, M.; Manes, A. Experimental and Numerical Evaluation of the Perforation Resistance of Multi-Layered Alumina/Aramid Fiber Ballistic Shield Impacted by an Armor Piercing Projectile. *Compos. Part B Eng.* **2022**, *230*, 109488. [CrossRef]

15. Sanjay, M.R.; Madhu, P.; Jawaid, M.; Senthamaraikannan, P.; Senthil, S.; Pradeep, S. Characterization and properties of natural fiber polymer composites: A comprehensive review. *J. Clean. Prod.* **2018**, *172*, 566–581. [CrossRef]

16. Neuba, L.M.; Pereira Junio, R.F.; Ribeiro, M.P.; Souza, A.T.; de Sousa Lima, E.; Garcia Filho, F.d.C.; Figueiredo, A.B.-H.d.S.; Braga, F.d.O.; Azevedo, A.R.G.d.; Monteiro, S.N. Promising Mechanical, Thermal, and Ballistic Properties of Novel Epoxy Composites Reinforced with *Cyperus malaccensis* Sedge Fiber. *Polymers* **2020**, *12*, 1776. [CrossRef]

17. da Luz, F.S.; Garcia Filho, F.d.C.; del-Río, M.T.G.; Nascimento, L.F.C.; Pinheiro, W.A.; Monteiro, S.N. Graphene-Incorporated Natural Fiber Polymer Composites: A First Overview. *Polymers* **2020**, *12*, 1601. [CrossRef]

18. Garcia Filho, F.D.C.; Oliveira, M.S.; Pereira, A.C.; Nascimento, L.F.C.; Matheus, J.R.G.; Monteiro, S.N. Ballistic behavior of epoxy matrix composites reinforced with piassava fiber against high energy ammunition. *J. Mater. Res. Technol.* **2020**, *9*, 1734–1741. [CrossRef]

19. Neuba, L.M.; Camposo Pereira, A.; Felipe Pereira Junio, R.; Teixeira Souza, A.; Soares Chaves, Y.; Picanço Oliveira, M.; Neves Monteiro, S. Ballistic Performance of *Cyperus malaccensis* Sedge Fibers Reinforcing Epoxy Matrix as a Standalone Target. *J. Mater. Res. Technol.* **2023**, *23*, 4367–4375. [CrossRef]

20. Braga, F.O.; Bolzan, L.T.; Lima, E.P.; Monteiro, S.N. Performance of natural curaua fiber-reinforced polyester composites under 7.62 mm bullet impact as a stand-alone ballistic armor. *J. Mater. Res. Technol.* **2017**, *6*, 323–328. [CrossRef]

21. Braga, F.O.; Bolzan, L.T.; Ramos, F.J.H.T.V.; Monteiro, S.N.; Lima, E.P., Jr.; da Silva, L.C. Ballistic efficiency of multilayered armor systems with sisal fiber polyester composites. *Mater. Res.* **2018**, *20*, 767–774. [CrossRef]

22. da Luz, F.S.; Monteiro, S.N.; Lima, E.S.; Lima Júnior, E.P. Ballistic application of coir fiber reinforced epoxy composite in multilayered armor. *Mater. Res.* **2017**, *20*, 23–28. [CrossRef]

23. Monteiro, S.N.; Candido, V.S.; Braga, F.O.; Bolzan, L.T.; Weber, R.P.; Drelich, J.W. Sugarcane bagasse waste in composites for multilayered armor. *Eur. Polym. J.* **2016**, *78*, 173–185. [CrossRef]

24. *NIJ 0101.06*; Ballistic Resistance of Body Armor. National Institute of Justice: Washington, DC, USA, 2008.

25. Demosthenes, L.C.d.C.; Luz, F.S.d.; Nascimento, L.F.C.; Monteiro, S.N. Buriti Fabric Reinforced Epoxy Composites as a Novel Ballistic Component of a Multilayered Armor System. *Sustainability* **2022**, *14*, 10591. [CrossRef]

26. Silva, D.S.; Junio, R.F.P.; Neuba, L.M.; Aguilera, L.S.; Monteiro, S.N.; da Silva, M.H.P. Thermochemical and structural characterization of raffia fiber fabric (Raphia vinifera) from the Amazon region. *J. Mater. Res. Technol.* **2024**, *30*, 5069–5079. [CrossRef]

27. Callister William, D.; Rethwisch, D.G. *Materials Science and Engineering: An Introduction*; John Wiley & Sons: Hoboken, NJ, USA, 2018; Volume 26.

28. Oliveira, M.S.; Garcia Filho, F.D.C.; Pereira, A.C.; Nunes, L.F.; da Luz, F.S.; Braga, F.O.; Colorado, H.A.; Monteiro, S.N. Ballistic performance and statistical evaluation of multilayered armor with epoxy-fique fabric composites using the Weibull analysis. *J. Mater. Res. Technol.* **2019**, *8*, 5899–5908. [CrossRef]

29. Swain, P.T.R.; Biswas, S. Physical and mechanical behavior of Al2O3 filled jute fiber reinforced epoxy composites. *Int. J. Curr. Eng. Technol.* **2014**, *2*, 67–71. [CrossRef]

30. Hamidi, Y.K.; Aktas, L.; Altan, M.C. Effect of packing on void morphology in resin transfer molded E-glass/epoxy composites. *Polym. Compos.* **2005**, *26*, 614–627. [CrossRef]

31. Huang, H.; Talreja, R. Effects of void geometry on elastic properties of unidirectional fiber reinforced composites. *Compos. Sci. Technol.* **2005**, *65*, 1964–1981. [CrossRef]

32. Manfredi, L.B.; Fraga, A.N.; Vázquez, A. Influence of the network structure and void content on hygrothermal stability of resol resin modified with epoxy–amine. *J. Appl. Polym. Sci.* **2006**, *102*, 588–597. [CrossRef]

33. He, Y.; Fan, X. In-situ Characterization of Moisture Absorption and Desorption in a Thin BT Core Substrate. In Proceedings of the 57th Electronic Components and Technology Conference, Sparks, NV, USA, 29 May–1 June 2007; pp. 1375–1383. [CrossRef]

34. Thomason, J.L. The interface region in glass fibre reinforced epoxy resin composites: 2. Water absorption, voids and the interface. *Composites* **1995**, *26*, 477–485. [CrossRef]

35. Fornari Junior, C.C.M. *Vegetable Fibers for Polymeric Composites*, 1st ed.; Editus UESC: Ilhéus-Bahia, Brazil, 2017; Volume 1, 198p.

36. Chee, S.S.; Jawaid, M.; Sultan, M.; Alothman, O.Y.; Abdullah, L.C. Accelerated weathering and soil burial effects on colour, biodegradability and thermal properties of bamboo/kenaf/epoxy hybrid composites. *Polym. Test.* **2019**, *79*, 106054. [CrossRef]
37. Kumar, R.; Ul Haq, M.I.; Sharma, S.M.; Raina, A.; Anand, A. Effect of water absorption on mechanical and tribological properties of Indian ramie/epoxy composites. *Proc. Inst. Mech. Eng. Part J J. Eng. Tribol.* **2022**, *236*, 1871–1879. [CrossRef]
38. Zeng, Q.; Lu, Q.; Zhou, Y.; Chen, N.; Rao, J.; Fan, M. Circular development of recycled natural fibers from medium density fiberboard wastes. *J. Clean. Prod.* **2018**, *202*, 456–464. [CrossRef]
39. Dittenber, D.B.; Gangarao, H.V.S. Critical review of recent publications on use of natural composites in infrastructure. *Compos. Part A Appl. Sci. Manuf.* **2012**, *43*, 1419–1429. [CrossRef]
40. Guo, Z.S.; Liu, L.; Zhang, B.M.; Du, S. Critical Void Content for Thermoset Composite Laminates. *J. Compos. Mater.* **2009**, *43*, 1775–1790. [CrossRef]
41. Costa, M.L.; Almeida, S.F.M.; Rezende, M.C. Resistência ao Cisalhamento Interlaminar de Compósitos com Resina Epóxi com Diferentes Arranjos das Fibras na Presença de Vazios. *Polímeros* **2001**, *11*, 182. [CrossRef]
42. Liu, L.; Zhang, B.M.; Wang, D.F.; Wu, Z.J. Effects of cure cycles on void content and mechanical properties of composite laminates. *Compos. Struct.* **2006**, *73*, 303. [CrossRef]
43. Liu, L.; Zhang, B.M.; Wang, D.F.; Wu, Z. Experimental characterization of porosity and interlaminar shear strength in polymeric matrix composites. *J. Aeronaut. Mater.* **2006**, *26*, 115.
44. Sreekala, M.; George, J.; Kumaran, M.; Thomas, S. The mechanical performance of hybrid phenol-formaldehyde-based composites reinforced with glass and oil palm fibres. *Compos. Sci. Technol.* **2002**, *62*, 339–353. [CrossRef]
45. Norizan, M.N.; Abdan, K.; Salit, M.S.; Mohamed, R.; Mara, M.U.T. Physical, mechanical and thermal properties of sugar palm yarn fibre loading on reinforced unsaturated polyester composites. *J. Phys. Sci.* **2017**, *28*, 115–136. [CrossRef]
46. Costa, U.O.; Nascimento, L.F.C.; Garcia, J.M.; Bezerra, W.B.A.; Monteiro, S.N. Evaluation of Izod impact and bend properties of epoxy composites reinforced with mallow fibers. *J. Mater. Res. Technol.* **2020**, *9*, 373–382. [CrossRef]
47. Marchi, B.Z.; Silveira, P.H.P.M.d.; Bezerra, W.B.A.; Nascimento, L.F.C.; Lopes, F.P.D.; Candido, V.S.; Silva, A.C.R.d.; Monteiro, S.N. Ballistic Performance, Thermal and Chemical Characterization of Ubim Fiber (*Geonoma baculifera*) Reinforced Epoxy Matrix Composites. *Polymers* **2023**, *15*, 3220. [CrossRef] [PubMed]
48. da Cunha, J.d.S.C.; Nascimento, L.F.C.; Costa, U.O.; Bezerra, W.B.A.; Oliveira, M.S.; Marques, M.d.F.V.; Soares, A.P.S.; Monteiro, S.N. Ballistic Behavior of Epoxy Composites Reinforced with Amazon Titica Vine Fibers (*Heteropsis flexuosa*) in Multilayered Armor System and as Stand-Alone Target. *Polymers* **2023**, *15*, 3550. [CrossRef] [PubMed]
49. Luz, F.S.d.; Junior, E.P.L.; Louro, L.H.L.; Monteiro, S.N. Ballistic test of multilayered armor with intermediate epoxy composite reinforced with jute fabric. *Mater. Res.* **2015**, *18*, 170–177. [CrossRef]
50. Monteiro, S.N.; Louro, L.H.L.; Trindade, W.; Elias, C.N.; Ferreira, C.L.; Lima, E.d.S.; Weber, R.P.; Suarez, J.C.M.; Figueiredo, A.B.-H.d.S.; Pinheiro, W.A.; et al. Natural Curaua Fiber-Reinforced Composites in Multilayered Ballistic Armor. *Metall. Mater. Trans.* **2015**, *46*, 4567–4577. [CrossRef]
51. Odesanya, K.O.; Ahmad, R.; Jawaid, M.; Bingol, S.; Adebayo, G.O.; Wong, Y.H. Natural Fibre-Reinforced Composite for Ballistic Applications: A Review. *J. Polym. Environ.* **2021**, *29*, 3795–3812. [CrossRef]
52. Harish, S.; Michael, D.P.; Bensely, A.; Lal, D.M.; Rajadurai, A. Mechanical property evaluation of natural fiber coir composite. *Mater. Charact.* **2009**, *6*, 44–49. [CrossRef]
53. de Assis, F.S.; Pereira, A.C.; da Costa Garcia Filho, F.; Lima, E.P., Jr.; Monteiro, S.N.; Weber, R.P. Performance of jute non-woven mat reinforced polyester matrix composite in multilayered armor. *J. Mater. Res. Technol.* **2018**, *7*, 535–540. [CrossRef]
54. Costa, U.O.; Nascimento, L.F.C.; Garcia, J.M.; Monteiro, S.N.; da Luz, F.S.; Pinheiro, W.A. Effect of graphene oxide coating on natural fiber composite for multilayered ballistic armor. *Polymers* **2019**, *11*, 1356. [CrossRef]